07.3

On the possible non-uniqueness of the conversion of laser radiation into electric current in multijunction monolithic photoconverters

© V.S. Yuferev, I.A. Tolkachov, V.S. Kalinovskii

Ioffe Institute, St. Petersburg, Russia
E-mail: valyuf@ammp3.ioffe.ru

Received July 5, 2023
Revised October 10, 2023
Accepted October 14, 2023

On the example of a two-junction monolithic photoconverter of laser radiation, the comparison of the complete model with a connective tunnel diode and a simplified model in which the tunnel diode is replaced by an electric coupling are performed. It is shown for the first time that for the same values of the problem parameters the complete model can have several solutions based on the tunneling and injection mechanisms of current flow through tunnel diodes. It is shown also that the simplified model gives smaller values of the short circuit current.

Keywords: photovoltaics, laser radiation, multi-junction photoconverter, tunnel diod.

DOI: 10.61011/TPL.2024.01.57831.19674

Recently, significant progress has been made in the conversion of laser radiation using vertical multijunction photoconverters (MPCs), which consist of epitaxially grown in monolithic form photoactive layers with a single $p-n$-junction (subconverters), arranged one above the other and connected in series by counter-connected tunneling diodes (TDs) [1,2]. Such devices allow to multiply the output voltage compared to single-junction photoconverters (PCs) and provide record high efficiency of optical-to-electrical power conversion. Due to these properties, the potential applications of MPCs are continuously expanding to include optical systems for wireless transmission of energy and information signals, radiophotonic devices as well as biomedical applications [3–5]. Numerical and experimental studies of MPC containing from 2 to 20$p-n$-junctions (see, e.g., [1,6–8]) have been reported in the literature, and the prospect of MPC with up to 100 [1] junctions has been substantiated. It should be noted that modelling MPC in a rigorous setting is not an easy task. The use of TCAD systems for this purpose often fails to produce positive results from for poor convergence. A possible reason is the need to numerically solve the charge carrier transport equations both in coupled tunnel diodes and in subconverters (SUBCON), and these problems are multiscale and require the use of meshes whose cell sizes may differ by several orders of [9] magnitude. On the other hand, if the current through the tunnel diode is less than the peak current, the TD behaves like an active resistance in terms of its electrical properties. This allows us to simplify the modelling of the MPC by dividing the problem into two: modelling of the TD and modelling of the photoconverter, in which the TDs are replaced by an electrical coupling (active resistance). This approach turns out to be very effective and is widely used in MPC modelling. However, the TDs have N--shaped current-voltage characteristic and hence have two stable equilibrium states. One corresponds to the process of tunneling of charge carriers through the TD barrier, and the other — the injection of charge carriers through this barrier as a result of its lowering. Accordingly, one can expect the appearance of several modes of current flow in the MPC, in particular, the existence of several load characteristics. To the best of our knowledge, this issue has not been addressed in the literature so far, different solutions have not been sought, and the matter has been limited to simply mentioning that in practice the tunneling mode is usually implemented. In addition, the question arises as to how different the computational results obtained using the full and simplified models can be. Answering these questions is the purpose of this paper.

Given the complexity of the MPC calculation, we limited ourselves to modelling the simplest GaAs-based two-stage PC. The process of interband tunneling was considered, which was taken into account by introducing an additional recombination term in the drift-diffusion equations using a nonlocal model [9]. Radiation was injected through the p-region. The wide-band window and rear barrier were absent to simplify the task. The structure parameters are summarized in the table. The choice of parameters was determined by the desire to demonstrate the peculiarities of the conversion of laser radiation into electric current using the full MPC model. The thicknesses of the subconverters were determined based on the condition of equality of the number of photons absorbed in each SUBCON. The absorption coefficient was taken to be $10^4\,\mathrm{cm}^{-1}$, and the incident power was $30\,\mathrm{W/cm}^2$, so that the current flowing through the PC was substantially less than the peak TD current. Shockley–Reed recombination and radiative recombination were taken into account. The processes of photon re-absorption were not considered.

Fig. 1 shows the calculated load characteristics of the PC. It can be seen that the full model indeed has two solutions. The curve *1* corresponds to the standard regime of current

Structure of a two-stage photoconverter

Material layer	Concentration donors N_D, cm^{-3}	Concentration acceptors N_A, cm^{-3}	Layer thickness$h$, μm
p-GaAs	–	$2 \cdot 10^{18}$	0.2
n-GaAs	$5 \cdot 10^{17}$	–	0.42
n^{++}-GaAs	$2 \cdot 10^{19}$	–	0.025
p^{++}-GaAs	–	$6 \cdot 10^{19}$	0.025
p-GaAs	–	$2 \cdot 10^{18}$	0.4
n-GaAs	$5 \cdot 10^{17}$	–	1.926

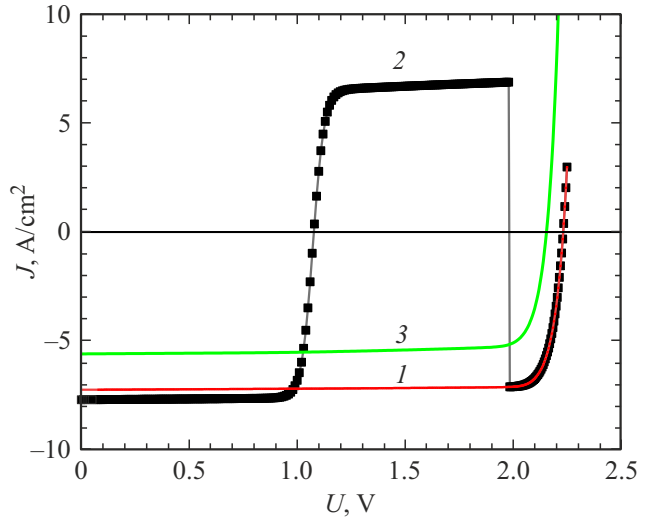

Figure 1. Load curves for two solutions under the full MPC model (*1*, *2*) and for the simplified model (*3*).

flow by tunneling through the TD barrier. In this case, the short circuit current $J_{sc} = -7.26\,\text{A/cm}^2$, the open circuit voltage $U_{oc} = 2.15\,\text{V}$, and the conversion efficiency is 42%. The second solution (curve *2*) corresponds to a slightly higher absolute value of $J_{sc} = -7.71\,\text{A/cm}^2$, but at voltage $U = 1.08\,\text{V}$ the current becomes equal to zero, and then with increasing voltage quickly reaches a value of 6.4 A/cm ^{2}, after which it remains almost constant. In this case, the driving force of the current is the voltage U, not the photovoltaic effect. At voltages above 2 V, the photovoltaic effect becomes dominant again, current becomes negative and this transition occurs abruptly and the two load curves appearing to coincide. The reason for this phenomenon is as follows. As the external voltage increases, the positive bias of the TD $p-n$-junction decreases and there is a corresponding shift to the left along the diffuse branch of the current-voltage characteristic of the TD. When the voltage drop across the TD reaches a value at which the diffuse branch is in contact with the unstable part of the current-voltage characteristic of the TD, a further decrease in this voltage causes a jump to another stable (tunnel) branch of the TD, which in turn causes a jump between the load curves. Fig. 1 also shows that in the simplified model, the short-circuit current is almost 30% lower (curve *3*). The latter is due to the fact that when the TD is replaced by electrical coupling, the SUBCON-TD boundary is replaced by an ohmic contact, which in this structure leads to the appearance of surface recombination at this boundary. By introducing a wide-band window and a rear barrier into each SUBCON, this effect may be weakened or even disappear in the simplified model.

Thus as expected N-shaped current-voltage characteristic of the tunneling diode can lead to the appearance of two modes of current flow in the two-junction PC, and, interestingly, their occurrence is not related to the current exceeding the peak value of the TD current. The first mode is associated with the tunnel branch of the current-voltage characteristic of the TD, and the second — with the diffusion branch, which corresponds to the injection of energetic charge carriers through the TD barrier as a result of the occurrence of a forward bias on it, greater than the voltage of the valley of the current-voltage characteristic of the TD. This can be clearly seen from Fig. 2, which shows the energy band diagrams calculated for the full and simplified models at zero external voltage. As would be expected, in both regimes a redistribution of the potential across the thickness of the PC occurred under the influence of radiation, with the result that each $p-n$-junction was shifted in either the forward or reverse direction. However, the pattern of shifts turns out to be significantly different. In the case of the first solution for the full model, as it can be seen from a comparison of the energy band diagrams with and without radiation (Fig. 2, *a* and *c*), a small positive bias occurs on the TD under illumination, corresponding to the tunnel branch of current-voltage characteristic, while the $p-n$-junctions of the first and second SUBCON are shifted in the positive and negative directions, respectively. The latter is due to the mismatch of currents in the subconverters. On the other hand, a similar comparison of the energy band diagrams for the second solution (Fig. 2, *b* and *c*) shows that in this case the first SUBCON is not shifted, while a positive bias of 1.15 V, close in magnitude to U_{oc} of the single-junction PC, appears on the TD and the second SUBCON. As the calculation results show, when the external voltage is increased, the situation does not change and the voltage at the second SUBCON remains close to 1.15 V, despite the reduction of the positive bias at the

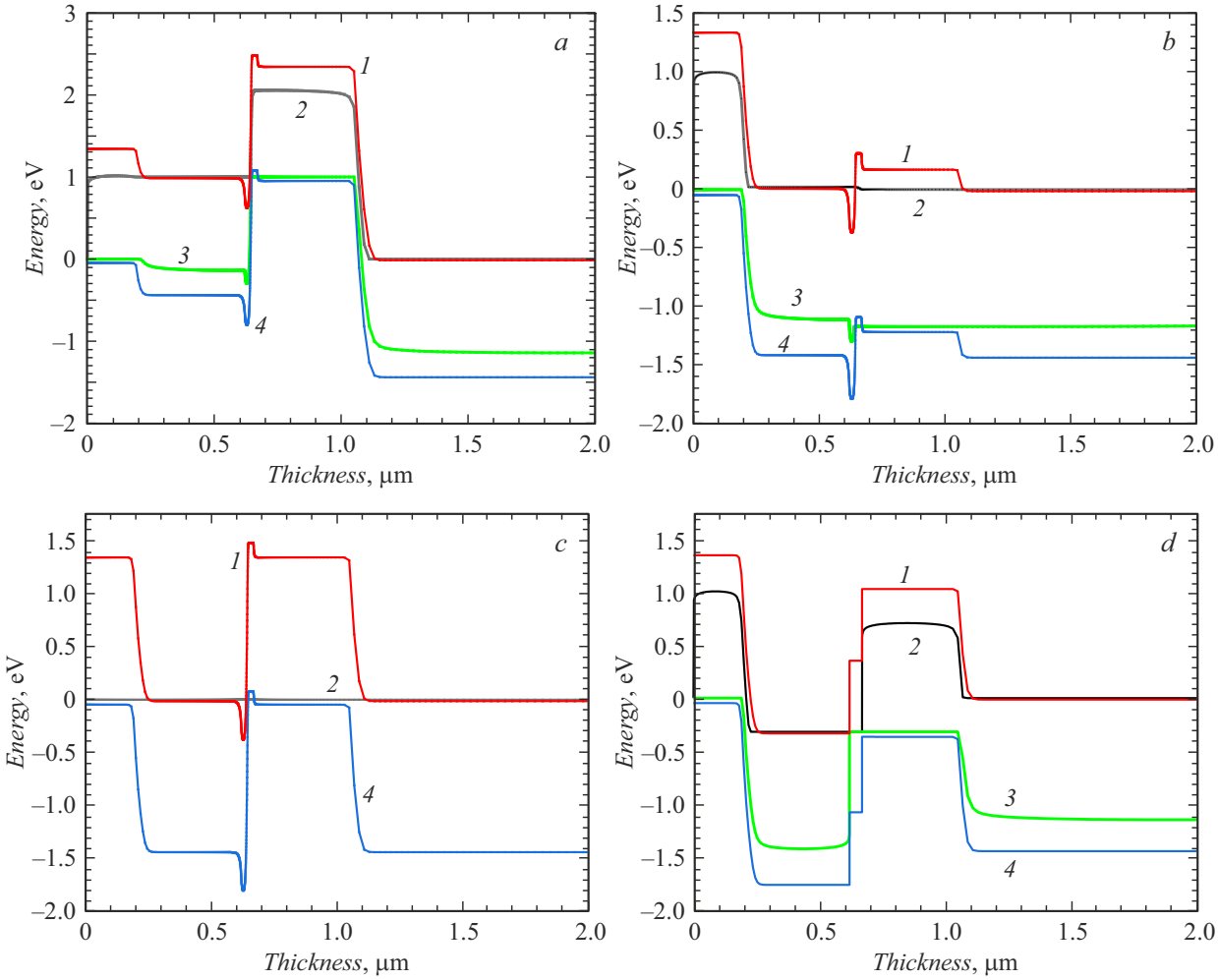

Figure 2. Energy band diagrams at zero external voltage for the full model (a–c) and the simplified model (d). a — the first solution, b — the second solution, c — the solution without radiation. *1* — bottom of the conduction band, *2* and *3* — quasi-Fermi levels for electrons and holes *4* — *4* valence band ceiling

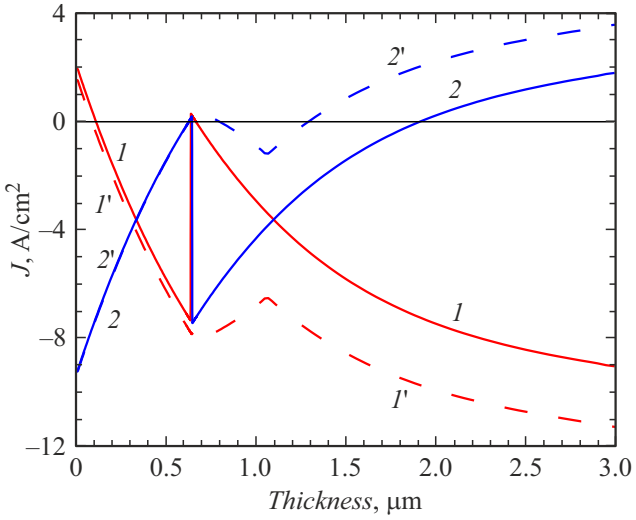

Figure 3. Distribution of electron (*1*, *1*') and hole (*2*, *2*') current densities along the thickness of the structure in the tunneling (solid curves) and injection (dashed curves) modes of current flow through the TD.

TD. This implies that the charge carriers generated in the second SUBCON do not contribute to the electric current; hence, in this regime, the two-junction PC operates as a single-junction one. Finally, we note that in the simplified model (Fig. 2, *d*) *p-n* junction of the first SUBCON shifts in the negative direction and the second — in the positive direction, i.e., the opposite of what occurs for the first solution in Fig. 2, *a*. Thus, although the same mode of current flow through the TD barrier is realized in both cases, the nature of the current mismatch between the SUBCON is found to be different in both models.

As another illustration of the differences between the solutions of the full model, the electron and hole current distributions along the thickness of the structure are shown in Fig. 3. It can be seen that in the tunneling mode of current flow there is a complete recombination of electrons and holes in the TD, and the electron and hole currents decrease almost to zero. In injection mode, this does not occur. Moreover, the positive voltage applied to the second SUBCON leads to such a strong weakening of the internal electric field that the hole current not only decreases

significantly, but also starts to flow in the opposite direction. At the same time, the electron current is determined by the electrons coming from the first SUBCON.

In conclusion, we note the following. First, there are all reasons to believe that the above is applicable to MPC with a greater number of $p-n$-junctions, and in second, the presence of two states of MPC suggests the possibility of creating a generator of electrical oscillations, the energy source of which is laser radiation.

Conflict of interest

The authors declare that they have no conflict of interest.

References

[1] M.C.A. York, S. Fafard, J. Phys. D: Appl. Phys., **50**, 173003 (2017). DOI: 10.1088/1361-6463/aa60a6
[2] S. Fafard, D.P. Masson, J. Appl. Phys., **130**, 160901 (2021). DOI: 10.1063/5/0070860
[3] H. Helmers, C. Armbruster, M. von Ravenstein, D. Derix, C. Schöner, IEEE Trans. Power Electron., **35**, 7904 (2020). DOI: 10.1109/TPEL.2020.2967475
[4] D.F. Zaitsev, V.M. Andreev, I.A. Bilenko, A.A. Berezovskii, P.Yu. Vladislavskii, Yu.B. Gurfinkel', L.I. Tsvetkova, V.S. Kalinovskii, N.M. Kondrat'ev, V.N. Kosolobov, V.F. Kurochkin, S.O. Slipchenko, N.V. Smirnov, B.V. Yakovlev, Radiotekhnika, **85** (4), 153 (2021) (in Russian). DOI: 10.18127/j00338486-202104-17
[5] P. Bhatti, Sci. Transl. Med., **7** (287), 287ec75 (2015). DOI: 10.1126/scitransalmed.aab3974
[6] J. Huang, Y. Sun, Y. Zhao, S. Yu, J. Dong, J. Xue, C. Xue, J. Wang, Y. Lu, Y. Ding, J. Semicond., **39** (4), 044003 (2018). DOI: 10.1088/1674-4926/39/9/094006
[7] A. Wang, J. Yin, S. Yu, Y. Sun, Appl. Phys. Lett., **121**, 233901 (2022). DOI: 10.1063/5.0109587
[8] S. Fafard, F. Proulx, M.C.A. York, L.S. Richard, P.O. Provost, R. Ares, V. Amez, D.P. Masson, Appl. Phys. Lett., **109**, 131107 (2016). DOI: 10.1063/1.4964120
[9] *Atlas User's Manual. Device simulation software* (Silvaco, 2015).

Translated by Ego Translating